sustainability

MDPI

Article

Characterization of the Coastal Vulnerability in Different Geological Settings: A Comparative Study on Kerala and Tamil Nadu Coasts Using FuzzyAHP

Chandra Shekhar Dwivedi [1], Shiva Teja Pampattiwar [1], Arvind Chandra Pandey [1], Bikash Ranjan Parida [1,*], Debashis Mitra [2] and Navneet Kumar [3]

[1] Department of Geoinformatics, School of Natural Resource Management, Central University of Jharkhand, Ranchi 835222, India
[2] Marine and Atmospheric Sciences Department, Indian Institute of Remote Sensing (IIRS), ISRO, Department of Space, Government of India, Dehradun 248001, India
[3] Department of Ecology and Natural Resources Management, Center for Development Research (ZEF), University of Bonn, 53113 Bonn, Germany
* Correspondence: bikash.parida@cuj.ac.in

Abstract: The acceleration of coastal processes is manifested in the form of coastal erosion, average sea level rise, drastic changes in coastlines, and more turbulent ocean waters. In this study, the coasts of Kerala and Tamil Nadu, India, were selected to identify the effects of increasing coastal processes. Therefore, it is necessary to identify and map vulnerable areas by taking into account the key parameters, such as topographical and socio-economic factors, to relate to coastal processes. The fuzzy Analytical Hierarchy Process (AHP) method was employed to identify the most vulnerable zones. The key findings revealed that about 14% and 2% of the coast of Tamil Nadu and Kerala, respectively, are classified under the physically highly vulnerable category. Similarly, ~17% and ~30% of coastal Tamil Nadu and Kerala, respectively, are highly socially vulnerable. The overall vulnerability assessment showed that 7–8% of both coastal areas were highly vulnerable. We concluded that the Thiruvallur, Chennai, Kanchipuram, Cuddalore, and Nagapattinam coasts on the east coast and the Malappuram, Thrissur, Ernakulam, Alappuzha, and Kollam coasts on the west coast were very highly vulnerable to coastal processes. Identifying vulnerable zones helps to better understand the impacts of rapid coastal processes and, with this prior estimation, the policymakers can take necessary actions to mitigate the irreversible impacts of coastal processes.

Keywords: coastal processes; vulnerability; fuzzy AHP; LRR; DSAS; wave watch III

Citation: Dwivedi, C.S.; Pampattiwar, S.T.; Pandey, A.C.; Parida, B.R.; Mitra, D.; Kumar, N. Characterization of the Coastal Vulnerability in Different Geological Settings: A Comparative Study on Kerala and Tamil Nadu Coasts Using FuzzyAHP. *Sustainability* **2023**, *15*, 9543. https://doi.org/10.3390/su15129543

Academic Editor: Ching-Piao Tsai

Received: 30 March 2023
Revised: 24 May 2023
Accepted: 8 June 2023
Published: 14 June 2023

1. Introduction

Coasts are always dynamic and are areas where land, water, and atmosphere interact with each other [1,2]. These interactions between the ecosystems lead to various processes occurring that affect every other coast differently. It is influenced by both topographic and hydro-dynamic changes occurring in the coastal and nearshore regions of the ocean where mass and energy are continuously being exchanged, resulting in the creation of a unique ecosystem [3]. These processes primarily affect the coastal geomorphology and geology and change that region by eroding, depositing, and inundating mass along the shore in the due course of action.

In the coastal process, all the participating factors can be divided into two different sets: coastal forcing/forces, which include waves, tides, sea level, surges, and currents that originate from different hydro-physical phenomena, such as sea level change, significant wave height, and tide range. These forces affect the second set, namely, coastal factors that comprise coastal geomorphology, geology, and elevation [4]. Coastal forces act on coastal factors, which result in coastal erosion and flooding, and may sometimes be severely affected by catastrophic surges and tsunamis [5–7]. Evaluating the impact of coastal processes on coastal areas requires continuous monitoring of processes and the retention of adequate records of events to analyze them all for research purposes. Real-time in situ monitoring from rider buoys and satellite data with good temporal coverage was found to be helpful in demarcating the changing land-water boundaries over time, from which many other indicators, such as the rate of change and the reason behind the change, can be obtained [8–10].

Coastal processes are changing a lot in these times as a consequence of global climate change [11]. The erosion of coasts, rise in mean sea level, and increased storminess of the ocean waters enhance coastal processes that lead to ecological changes along the coasts [12]. These enhanced coastal processes produce a list of coastal changes, including shore erosion, strong storm surges, an increase in significant wave height, an increase in sea level rise, and cyclonic activity, impacting the coast both geographically and economically [3,13,14]. Coastal systems are increasingly threatened by the potential impacts of climate change, according to a series of assessments by the Intergovernmental Panel on Climate Change (IPCC). On a global scale, climate change is causing sea levels to rise at higher annual rates as an impact of melting glaciers and ice caps on the Earth, which is happening due to a rise in pollution and global warming [15]. According to the measurements recorded at tide stations installed globally, a rise in sea level can be observed from 1 mm to 2 mm annually over the past century, which can be attributed to global warming [16]. Unfortunately, these areas are also exposed to natural disasters, such as coastal erosion, storm surge attacks, and coastal flooding. As a result of global warming, coastal cities are becoming increasingly susceptible to flooding [4].

Coastal vulnerability, which has been studied for a long time [17], refers to the condition of a selected area prone to the impact of increased coastal processes [18]. Specifically, the Coastal Vulnerability Index (CVI) has been widely used by combining physical and socio-economic variables for different coastal areas worldwide, viz., the U.S. coast, Australian coast, African coast, Indian coast, and European coast [19]. Typically, geological (e.g., geomorphology, shoreline erosion/accretion rates, coastal slope, emerged beach width, artificial protection structures, and dunes), hydro-physical processes (i.e., river discharge, sea level change, mean significant wave height, and mean tide range), and vegetation (e.g., land use and land cover types) variables are mostly used to derive CVI [19]. In India, the National Centre for Ocean Information Services (INCOIS) has assessed coastal vulnerability for the entire Indian coast, and the corresponding CVI atlas was available at 1:1,00,000 scale that used parameters such as tidal range, wave height, coastal slope, coastal elevation, shoreline change rate, geomorphology, and historical rate of relative sea level change [20]. Studies have also used physical and socio-economic (e.g., gender, age, income, population density, and tourist density) variables to estimate CVI and the Social Vulnerability Index (SVI) over coastal areas for coastal disaster management and building resilient coastal communities [21]. Researchers have developed different approaches to estimate and identify vulnerable zones in coastal regions impacted by different coastal forces [22]. The InVEST (Integrated Valuation of Ecosystem Services and Tradeoffs) coastal vulnerability model has been applied to estimate the degree of coastal vulnerability based on several variables [23,24]. The Multi-Dimensional Coastal Vulnerability Index (MDim-CVI) combines a composite set of physical, environmental, and socio-economic indicators to deduce coastal vulnerabilities and changes in the environmental and socio-economic systems in the Italian coasts [25]. Multi-Criteria Decision Making (MCDM) models, such as the Analytical Hierarchy Process (AHP), Fuzzy AHP, fuzzy logic, and Technique for Order Performance by Similarity to Ideal Solution (TOPSIS) are widely used to deduce coastal vulnerabilities, each of which has its advantages and disadvantages [5,8,26]. Decision-making models such as AHP are used when the decision maker is sure about the phenomena and the phenomena are not about to change for a long or considerable period. Among these techniques, the results of the fuzzy AHP method are reported to be accurate and reliable, which is due to its computing process. In computing the fuzzy AHP, the decision maker has a wide range of options to choose the possible outcome of the phenomena. The fuzzy logic-based geospatial normalization technique has been applied based on several factors (i.e., coastal characteristics, coastal forcing, and socio-economic) for coastal vulnerability analysis of the Bangladesh coast [27–32].

The Indian coast can be divided into two major parts, i.e., the east coast and the west coast [15]. The difference between the east and west coasts of India can be seen based on the geology of the coasts and shores on either side [16]. The east coast is sandy and the west coast is more or less rocky, which further indicates that the east coast of India is more vulnerable to coastal processes, whereas the western coastal regions are somewhere still rigid to coastal forcing [17]. Apart from different geological settings, the west coast and the Western Ghats are home to many endangered species of flora and fauna [33,34]. At the same time, the east coast of the study area has heavy commercial and economic activities because of the presence of ports and large cities along and near the coast [35]. Several anthropogenic activities occur in coastal areas, and climate change increases the intensity of coastal hazards [1,10,36]; therefore, this study aims to estimate the coastal vulnerability in different geological settings to climate change impacts and to provide a comparative assessment of both coasts. Very few studies have dealt with the applicability of the fuzzy AHP to estimate coastal vulnerability, such as physical, social, and overall vulnerabilities. Hence, the objective of the present study was to develop a comparative vulnerability assessment between two different coasts by studying and identifying the responsible coastal processes posing threats to the area selected by incorporating fuzzy AHP for the estimation of coastal vulnerability. In this paper, Section 2 describes the study area, Section 3 discusses materials and methods (i.e., coastal vulnerability assessment), Sections 4 and 5 describe the results and discussion, respectively, followed by the conclusion in Section 6.

2. Study Area

For this study, two coasts with different characteristics were selected, which are the southern margins of India, i.e., the coasts of Kerala and Tamil Nadu, surrounded by the Arabian Sea in the west and the Bay of Bengal in the east. Both coastlines lie between 8° N to 13° N, and 75° E to 80° E, sharing boundaries with the Indian Ocean in three different directions and as a part of the subcontinent from the northern side (Figure 1). In this study, it was noticed that political district boundaries were not suitable for considering them as the study area due to the irregularity of their shape. At the same time, coastal processes have no impact on many parts, as they are continuing their extent towards the mainland rather than running parallel to the shoreline. To resolve this issue, only the seaward sides of the coastal districts were considered.

The study area map is shown in Figure 1 where a 40 km buffer was created from the Tamil Nadu shoreline and a 35 km buffer was created from the Kerala shoreline towards the mainland using the buffer tool. We considered these two polygons as the primary study area. Upon observing the satellite images, the hilly topography is observable on both coasts, but the Eastern Ghats are slightly discontinuous and far from the shore, whereas the Western Ghats are continuous and comparatively near the shore. Hence, a 40 km buffer on the east and a 35 km buffer on the west were created. These two polygons were merged, and their area statistics are mentioned. The 40 km wide region along the Tamil Nadu shoreline has an area of 31,842.3 km^2, whilst the 35 km wide region parallel to the Kerala shoreline has an area of 19,405.3 km^2. The total area is 51,247.6 km^2, which includes both the Tamil Nadu and Kerala coasts. The detailed statistics for each coastal district are given in Table 1.

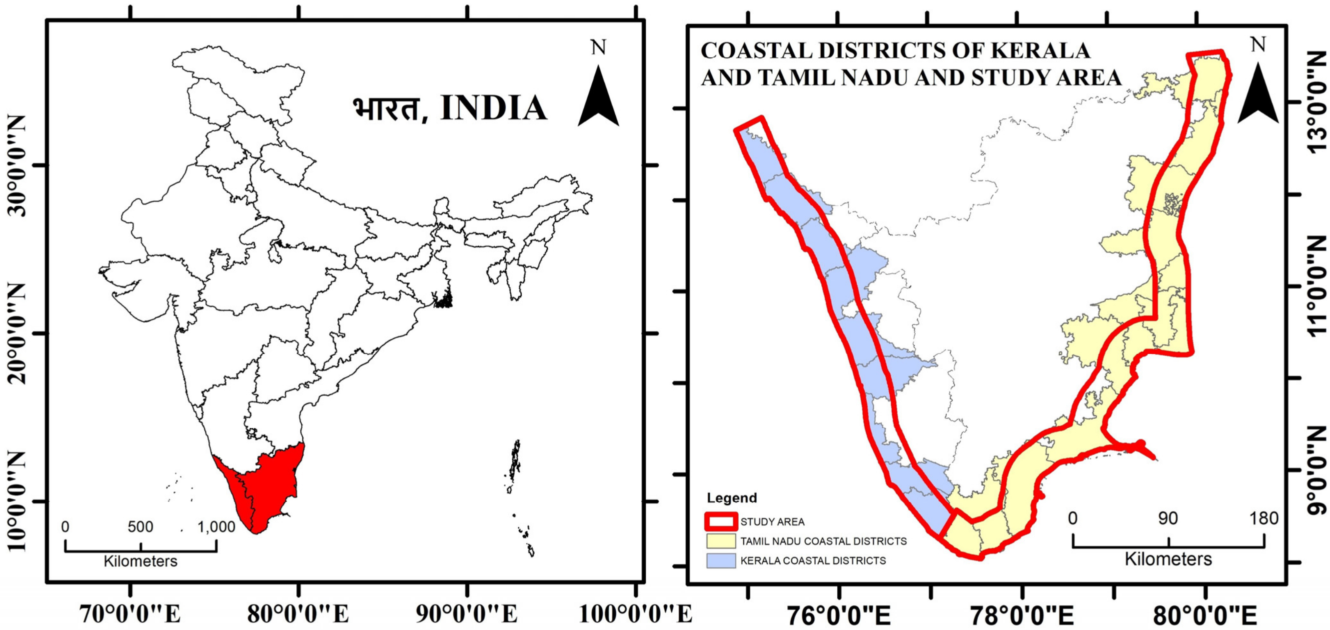

Figure 1. Study region is highlighted in the India map (**left**) and the buffer of the average coast is shown on the **right** side.

Table 1. Study area statistics such as state name, district name, east–west extent, and coastal extent.

State	SL. NO	Coastal District	East West Extent (km)	Coastal Extent (East/West) (km)
TAMIL NADU	1	THIRUVALLUR	118	E 59
	2	CHENNAI	18	E 9
	3	CHENGALPATTU	50	E 25
	4	VILLUPURAM	90	E 45
	5	CUDDALORE	100	E 50
	6	MAYILDATURAI	36	E 18
	7	NAGAPATTNAM	65	E 32.5
	8	THANJAVUR	90	E 45
	9	PADUKOTTAI	108	E 54
	10	RAMANATHAPURAM	140	E 70
	11	THOOTHUKUDI	98	E 49
	12	THIRUNELVELI	96	E 48
	13	KANYAKUMARI	59	E 29.5
		AVERAGE	82.15	41.08
KERALA	14	KASARAGOD	38	W 19
	15	KANNUR	80	W 40
	16	KOZHIKODE	56	W 28
	17	MALLAPPURAM	88	W 44
	18	THRISSUR	98	W 49
	19	ERNAKULAM	98	W 49
	20	ALAPPUZAH	30	W 15
	21	KOLLAM	75	W 37.5
	22	THIRUVANANTHAPURAM	72	W 36
		AVERAGE	70.56	35.28

3. Materials and Methods

The datasets used in this study are described in Table 2, which includes satellite data and various parameters used to deduce coastal vulnerability. The parameters used for coastal vulnerability include geological (e.g., geomorphology, shoreline erosion/accretion rates, and coastal slope) and hydro-physical processes (i.e., sea level change, mean significant wave height, and mean tide range), and socio-economic factors (e.g., urban density, rural density, and population density). Landsat is a multispectral open-source satellite series operating under the United States Geological Survey (USGS) [37,38]. Its Level 2 (Collection 1) surface reflectance data were downloaded to help identify coastal landforms and shorelines easily. In this study, bands 4, 3, 2, and 1 of Landsat-5, and bands 5, 4, 3, and 2 of both Landsat-8 and 9 were used for the years 1990–2022 with 5 years intervals. The Shuttle Radar for Topographic Mission (SRTM) [39,40] uses the C and X bands, where C is for space-borne imaging and X is used for its Synthetic Aperture Radar (SAR) to make it an interferometric radar. It compares two different radar signals and forms one single image. Out of its three products, SRTM 1 arcsec global data were used because of its resolution, which is similar to that of Landsat data.

Table 2. Data used to assess the coastal vulnerability.

Dataset	Source	Type	Resolution	Year	Month
Landsat 5, 8, and 9	USGS	MSS Raster	30 m	1990–2022	Nov–Dec
Geomorphology 1:250 K	Bhukosh GSI	Shapefile	250 m	2015	-
SRTM	Earthdata	Geo tiff	30 m	2000	-
WAVE WATCH III	APDRC	NetCDF	3 h	1997–2019	Annual
GLOSS–PSMSL	PSMSL	Text	-	1990–2020	Annual
Population	SEDAC	Raster	1 km	2011	-
Built-up	SEDAC	Shapefile	250 m	2011	-

The Geological Survey of India (GSI) provides different types of processed geospatial data on its official portal (bhukosh.gsi.gov.in) [41]. Wave Watch III is an open-source dataset that is freely available from the Asia Pacific Data Research Centre. It has six products, [42,43] out of which the surface significant wave height data were downloaded and processed for mapping. The SRTM-based Digital Elevation Model (DEM) was used to derive the slope. The slope was also considered as a parameter for vulnerability. The Global Sea Level Observation System (GLOSS), established in 1985 by the Intergovernmental Oceanographic Commission (IOC), is a high-quality on-site sea level system that supports a broad research and operational user base [43–45]. GLOSS monitors and provides global and regional sea level networks in support and guidance of the oceanography and climate research communities. These data are openly accessible, and, in this study, the data from five tide stations were used to map the rising sea levels.

The Socio-Economic Data and Application Centre (SEDAC) is an open-access socio-economic and demographic database that provides the population of India, with a resolution of 1 km based on the 2011 census [46]. A raster format of the population helps in choosing minute or irregularly shaped study areas, and the exact number of people falling in and becoming affected can be easily mapped and estimated. SEDAC also provides a shapefile for built-up classes, such as urban and rural built-up, based on global standards [46]. The population density of SEDAC shows the population per pixel based on the Census India 2011 dataset. The second parameter considered for social vulnerability is the built-up density. Physical vulnerability is also considered as the third parameter in order to assess its impact on different social conditions. The other and final parameter taken into consideration was urban density to establish a connection between urban and physical vulnerability and other social factors that affect vulnerability.

The regional elevation was obtained from SRTM, and the classification of elevation was performed based on earlier studies in the same or similar regions. The classification scheme used by Basheer [11,47] for regional elevation was considered as it was suitable for the selected study area. In this case, the class intervals for elevation were ≤ 0, 1–10 m, 10–20 m, 20–30 m, and >30 m. Typically, various coastal processes influence the coast up to 50 m. In the worst case, regions below 0 m are more vulnerable than regions at a certain altitude.

Significant wave height data were obtained in NetCDF file format from the WaveWatch III dataset. R Studio was used to compute the daily, monthly, and annual averages. The annual averages from 1997 to 2019 were converted from raster to points using ArcMap. Using the converted points, interpolation was performed using the kriging tool. Using the obtained grid, a significant wave height map was made using the appropriate map attributes. The significant wave height was classified under 4 classes, namely, classes carrying waves of 0.9–1.2 m in the "High" class, followed by 0.6–0.9 m in the "Moderate" class, 0.3–0.6 m in the "Low" wave height class, and less than 0.3 m in the "Very Low' class. In the study area, only one class of very high significant wave height was identified as per the standard classification.

Sea level rise is a concerning issue that contributes significantly to coastal disasters, such as storm surges, coastal flooding, seawater intrusion, and coastal erosion [11,48–51]. To understand sea level trends, mean sea level (PSMSL) data and mean sea level rider buoy data from the GLOSS observatories were obtained. Rider buoys can be found along the coast in key locations, such as Chennai, Thangachimadam, Nagapattinam, Kollam, and Mangalore. All data were processed using spreadsheets to obtain data at monthly intervals.

The digitized shorelines were converted to KML (Keyhole Mark-up Language) files and overlaid on Google Earth Pro's high-resolution temporal satellite imagery. These shorelines were processed and a Linear Regression Rate (LRR) was calculated among shorelines from 1990 to 2022 using Digital Shoreline Analysis Software (DSAS). The uncertainty parameter was set to ± 10 m. The result of the LRR was classified into 5 classes: very high erosion, high erosion, no change, high accretion, and very high accretion. To derive shoreline behavior, the number of transects falling in each class was noted down, and their total distance was calculated based on the transect spacing. Here, the incorporated transect spacing was 50 m. Based on the class-wise transect distribution, the shoreline behavior was easily identifiable. As the LRR incorporates every shoreline, unlike End Point Rate (EPR) or Net Shoreline Movement (NSM), the results are more appropriate and reliable.

The methodology flowchart is illustrated in Figure 2, which was used to obtain physical vulnerability, social physical vulnerability, and overall physical vulnerability. Geometric corrections were applied to the Landsat images and were used to digitize and extract shorelines, as well as to identify different coastal landforms and cross-check with the predefined geomorphology by the GSI. Using both Landsat datasets and geomorphology at a 1:250,000 scale, a major geomorphology map was prepared with classes, namely young and old coastal plains, deltaic and flood plains, and pediment complexes.

Coastal Vulnerability Assessment

In this study, coastal vulnerability was derived in three stages: (i) physical vulnerability, (ii) social vulnerability, and (iii) overall vulnerability. For assessing physical coastal vulnerability, physical parameters such as geomorphology, elevation, mean sea level rise, significant wave height, tidal range, and shoreline behavior were considered. A pairwise comparison matrix was developed using fuzzy triangular numbers ranging from 1 to 9 (Tables 3–5) with three in a set, such as either equal or an increasing order from left to right. In the case of social vulnerability, parameters such as population density, urban and rural densities, and built-up densities were considered and used for the fuzzy AHP calculations. Using a pairwise comparison matrix and a normalized matrix (Appendices A and B), the weights were calculated for each parameter. The obtained weights are said to be correct if the consistency ratio is less than 0.10 (Appendix C), and the weights can be assigned in the vulnerability mapping. The derived weights were validated by the calculation of Consistency Index (CI) and Consistency Ratio (CR) values (Appendix D). To map the physical vulnerability, all the maps of selected physical parameters were first converted to shapefile format while keeping the same intervals as calculated in the fuzzy AHP matrixes. The derived weights were added as attributes to the shapefiles and were further converted into rasters. These can be termed as "weighted rasters". All of these weighted rasters were run through the fuzzy membership tool one by one, making rasters ready for the fuzzy overlay. Finally, the fuzzy overlay tool was used to overlay all the weighted rasters and derive the output as physical or social vulnerability. After obtaining the physical and social vulnerabilities, both were averaged using the raster calculator, and the final overall vulnerability map was made. The process of the fuzzy AHP calculation and vulnerability derivation is graphically shown in Figure 3.

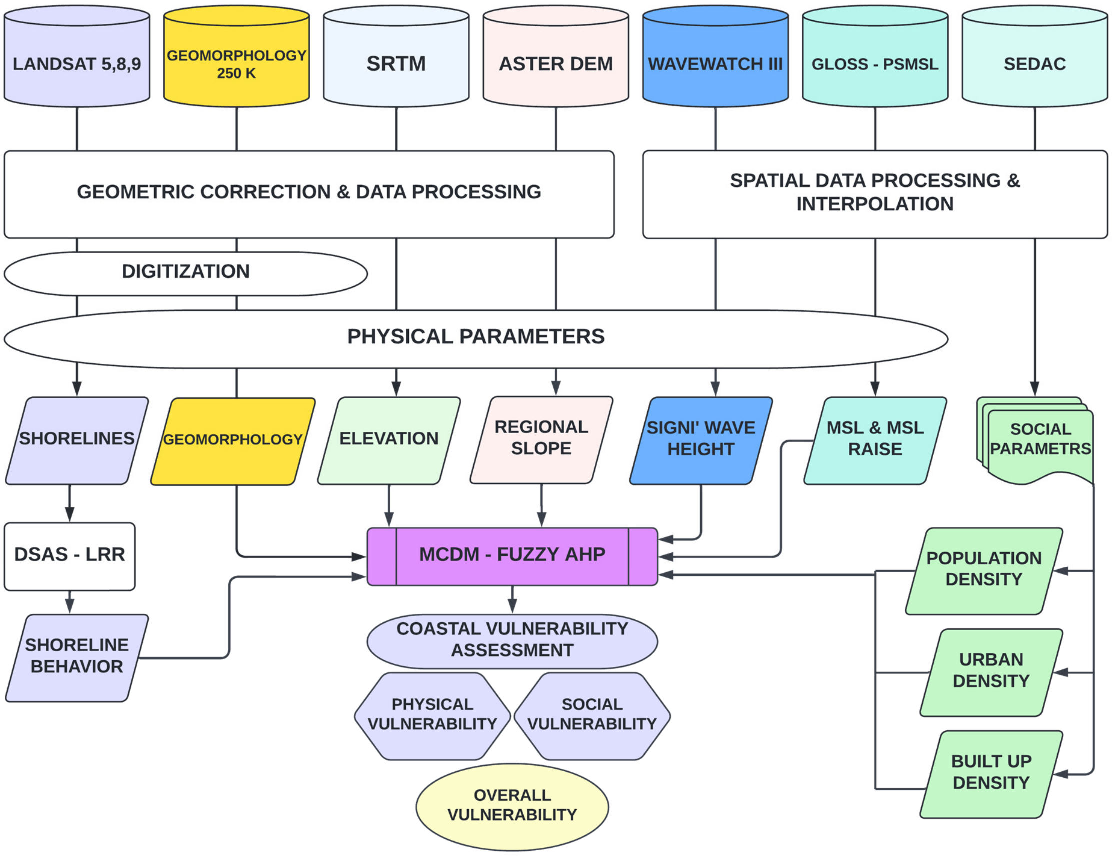

Figure 2. Methodology flowchart indicating steps to compute coastal vulnerability.

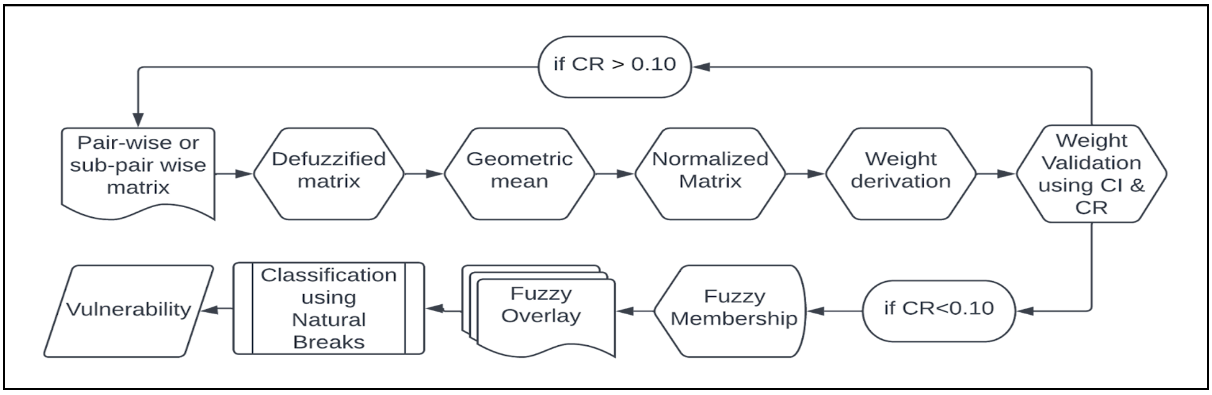

Figure 3. Process of estimating vulnerability using fuzzy AHP.

Table 3. Pair-wise matrix for physical vulnerability assessment.

Parameter	Geomorphology (GEO)			Regional Elevation (RE)			Mean Sea Level Rise (MSL)			Surface Sig' Wave Height (SWH)			Slope			Shoreline Movement (SM)			Weights
GEO	1	1	1	1	1	2	2	3	4	9	9	9	7	8	9	7	8	9	0.37066
RE	0.5	1	1	1	1	1	4	5	6	4	5	6	7	8	9	7	8	9	0.33066
MSL	0.25	0.33	0.50	0.17	0.20	0.25	1	1	1	2	3	4	2	3	4	6	7	8	0.13829141
SWH	0.11	0.11	0.11	0.17	0.20	0.25	0.25	0.33	0.50	1	1	1	2	3	4	4	5	6	0.082198
Slope	0.11	0.13	0.14	0.11	0.13	0.14	0.25	0.33	0.50	0.25	0.33	0.50	1	1	1	1	1	2	0.038915
SM	0.11	0.13	0.14	0.11	0.13	0.14	0.13	0.14	0.17	0.17	0.20	0.25	0.5	1	1	1	1	1	0.030868

Table 4. Sub-pair-wise matrix for vulnerability assessment.

Scale	Very High Vulnerability (VHV)			High Vulnerability (HV)			Medium Vulnerability (MV)			Low Vulnerability (LV)			Very Low Vulnerability (VLV)		
VHV	1	1	1	1	1	2	2	3	4	4	5	6	7	8	9
HV	0.5	1	1	1	1	1	2	3	4	4	5	6	7	8	9
MV	0.25	0.33	0.50	0.25	0.33	0.50	1	1	1	2	3	4	4	5	6
LV	0.17	0.20	0.225	0.17	0.20	0.25	0.25	0.33	0.50	1	1	1	2	3	4
VLV	0.11	0.13	0.14	0.11	0.13	0.14	0.17	0.20	0.25	0.25	0.33	0.50	1	1	1

Table 5. Classification scheme under different classes. The shoreline behavior and population density are abbreviated as SB and PD, respectively.

Parameter	VHV	HV	MV	LV	VLV
GEO	Coastal plain	Deltaic plain	Flood plain	Water bodies	PPC and hills
RE	<3 m	4 to 6 m	7 to 12 m	12 to 18 m	>18 m
SLR	>3.16 cm	2.96 to 3.16 cm	2.51 to 2.95 cm	1.81 to 2.5	<1.8 cm
SWH	>1.2 m	0.9 to 1.2 m	0.6 to 0.9 m	0.3 to 0.6 m	<0.3 m
Slope	0–10 degrees	10–20 degrees	20–45 degrees	45–60 degrees	60–89 degrees
SB	Very high erosion	High Erosion	High Accretion	VH Accretion	No Change
PD	>1000 ppl/km^2	500–1000	250–500	100–250	<100
Built-up density	80–100%	40–80%	20–40%	10–20%	<10%
Urban density	>400 hh/km^2	200–400	100–200	50–100	<50

$$A^k = aij^k = \begin{bmatrix} 1 & a12^k & \cdots & a1n^k \\ a21^k & 1 & \cdots & a2n^k \\ \vdots & \vdots & \vdots & \vdots \\ an1^k & an2^k & \cdots & 1 \end{bmatrix}$$

The above formula describes the pairwise comparison matrix as a deriving method using different experts. The pairwise comparison matrix between criterion *i* and criterion *j* of each expert *k* is shown below.

$$A^k = \frac{1}{aij^k} \quad i > j$$

where a_{ij} is used to derive the judgment of the decision makers. For further information, one should refer to Tahri [5].

4. Results

In this section, we described hydro–geographic parameters (geomorphology, regional elevation, surface significant wave height, mean sea level rise, regional slope, and shoreline behavior using linear regression rate) and socio-economic parameters (regional population density, regional built-up area and urban density) followed by physical vulnerability assessment, social vulnerability assessment, overall vulnerability assessment, and finally the comparative assessment between Tamil Nadu and Kerala coasts.

4.1. Hydro–Geographic Parameters

4.1.1. Mean Sea Level Rise

The monthly sea level rise exhibited that the study area experienced only two ranges of sea level rise. Less than 1.8 mm changes were observed on the majority of the east coast, whereas sea level rise between 1.81 and 2.5 mm was seen along the Kerala coast and the northern Tamil Nadu coast (Figure 4). The above classification is adopted from a study by Naga Kumar [47]. As shown in Figure 4, the highest sea level rise was found on the west coast at Mangalore, followed by Kochi, Chennai (east), and further followed by Tuticorin and Thangachimadam, respectively.

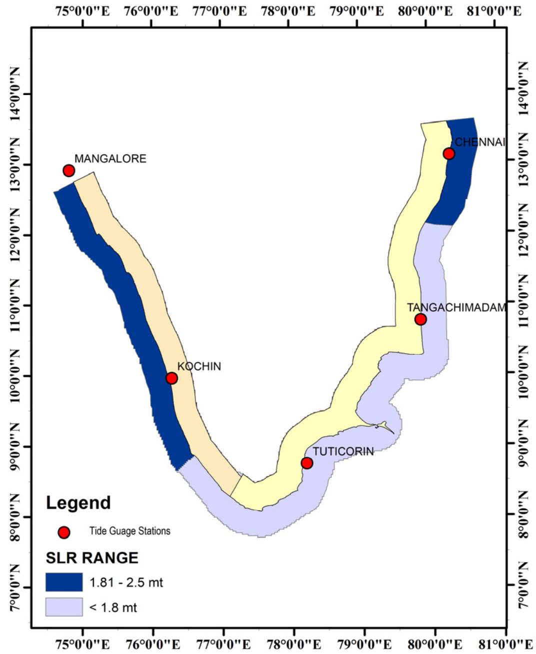

Figure 4. Display of sea level rise using PSMSL–GLOSS data.

4.1.2. Geomorphology

A large extent of the study area is situated within the geomorphology of the coastal plains, followed by the deltaic plains and the pediment–pediplain complex (Figure 5a). So, the area of the geomorphology will not decide the exposure to damage; rather, the threat of exposure is dependent on the nature of the soil and geological composition. On the east coast, the shoreline is mostly covered by coastal plains, which can be seen in the less-developed eastern regions of Cuddalore, Nagapattinam, and Ramanathapuram. In the west, the coastal plains, especially the younger coastal plains, occupy large areas along with flood plains and can be seen in the regions of Alappuzha, Thrissur, Malappuram, etc. The majority of the Kerala coast is covered by a combination of pediment complexes and structural hills. The percentage-wise geomorphological composition showed that more than half of the study area is covered by pediplain complex and hilly regions at 57.15%, followed by deltaic plains at 17.78%, coastal plains at 13.14%, water bodies such as rivers, lakes, dams, and reservoirs at 6.99%, and lastly by flood plains at 4.93%. Due to the presence of the Western Ghats very near the coastal area with a marginal distance of 30–35 km from the seashore, the western part of the coast is less vulnerable than the eastern coast. The Eastern Ghats, though present, are discontinuous and a little far from the seashore, creating sufficient space between the foothills of the Eastern Ghats and the sea to form a mixture of landforms.

4.1.3. Regional Elevation

After the regional elevation classification, the seaward margins of regions such as Thiruvallur, Chennai, Cuddalore, Kanchipuram, Villupuram, Nagapattinam, Ramanathapuram, and Thoothukudi fell under very low and low elevated areas on the east coast. The sea sides of Alappuzha, Malappuram, and Thrissur, followed by the Kollam and Kannur regions on the west coast, are classified as low-lying or very low-lying (Figure 5b). The spatial extent based on classification states that more than half, i.e., 25,705.51 km^2, is under the class of more than 18 m, followed by the moderate class with 10,044.6 km^2 under 7–12 m, 7372.2 km^2 in the low elevated class of 4–6 m, 5429 km^2 is under the 12–18 m class, and lastly, the least area is occupied by the very low-lying area class, i.e., <3 m with 1792 km^2.

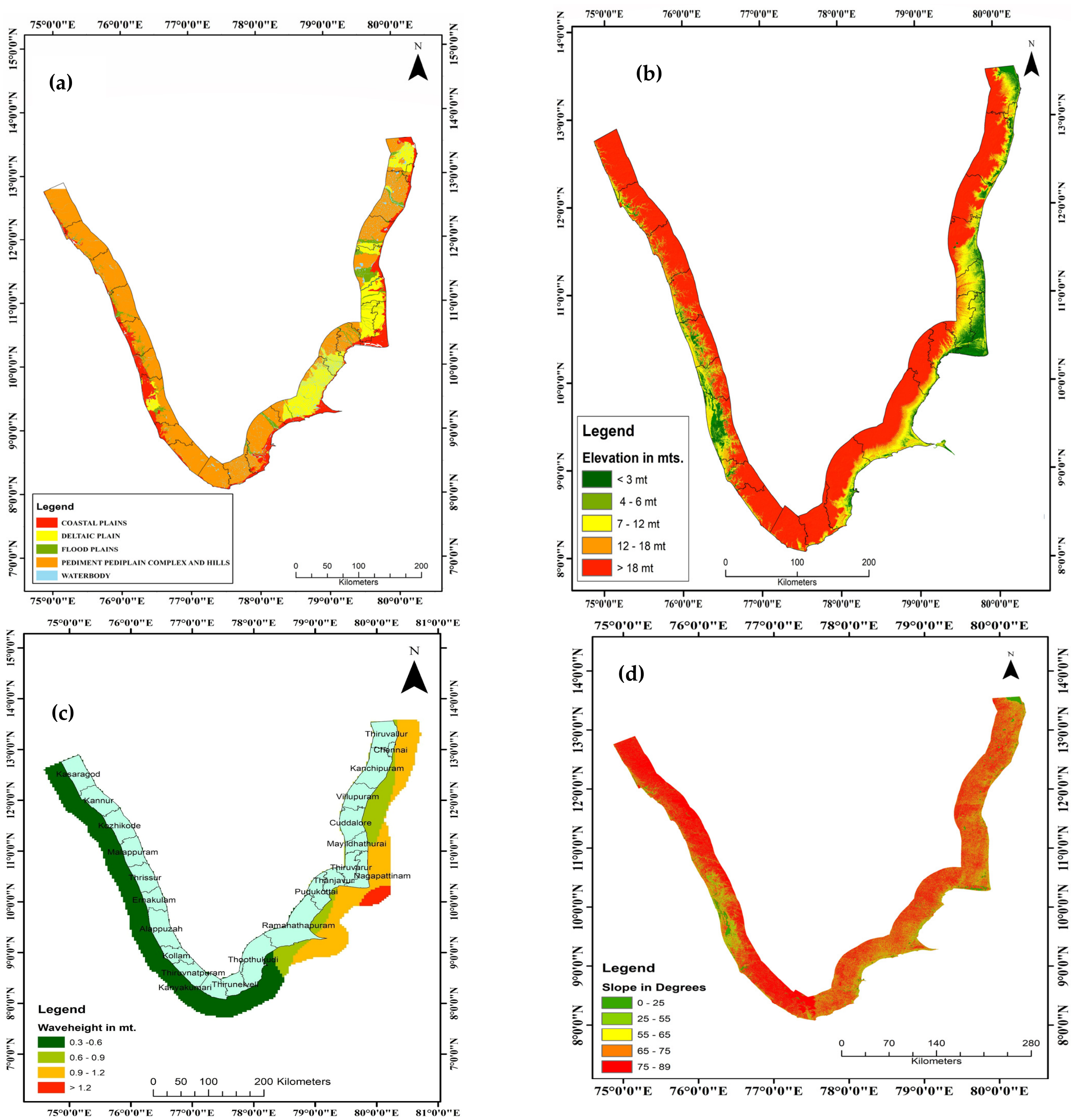

Figure 5. Displays different physical parameters such as (**a**) geomorphology, (**b**) regional elevation, (**c**) surface significant wave height, and (**d**) regional slope.

4.1.4. Surface Significant Wave Height

Based on surface significant wave height classification (Figure 5c), it can be seen that the Kerala coast receives comparatively low-height waves from the Tamil Nadu coast. On this map, the entire west coast lies in very low waves, and the regions of Thoothukudi, Ramanathapuram, Villupuram, and Cuddalore lie in low-wave regions. The Chennai and Thiruvallur regions fall under the moderate class, and the Nagapattinam region experience very high wave heights.

4.1.5. Regional Slope

The slope map (Figure 5d) shows that regions such as Alappuzha and Malappuram on the west coast and Nagapattinam on the east coast have slopes of less than 20°. The very high degrees of slopes, i.e., from 80 to 89°, can be seen in the western parts of the study area continuing until Kanyakumari of Tamil Nadu. This is because of the presence of the Western Ghats very near the coastal areas. At the same time, the eastern coast lies in the range of moderate slopes ranging from 40 to 60°, as shown in yellow and orange colors. The low slope visible on the top north of the east coast is the Pullicat Lake, sharing a boundary with the shoreline.

4.1.6. Shoreline Behavior using Linear Regression Rate

Based on the LRR analysis of the shorelines (Figure 6), the number of transects in each district in each class was identified. Based on the quantity, the length of the shoreline in each class was calculated. The total number of transects on the Kerala shoreline was 1167 (at 50 m intervals), out of which 35 were under very high erosion, 177 were under high erosion, 598 under no change, 340 under high accretion, and 17 were experiencing very high accretion. Nearly 17.5 km of the Kerala shoreline was found under very high accretion, which accounted for 3% of the entire shoreline. In the same way, an 8.5 km shoreline was found under very high accretion and accounted for 1.46% of the shoreline. As a result, Thrissur, Thiruvananthapuram, and Alappuzha districts were found to be very highly eroded and the shores of Kozhikode district were found to have very high accretion (Figure 7a). Similar results could be seen on the shores of Tamil Nadu. The total number of transects was 1815 (at 50 m spacing) and formed 908 km, out of which 107 transects fell under the very high erosion class, 405 under high erosion, 983 under no change, 273 under high accretion, and 47 under very high accretion (Figure 7b). About 5.9% (i.e., 53.5 km) of Tamil Nadu's shoreline was under very high erosion, 23.3% under high erosion, 54.16% under no change, 15.04% under high accretion, and 2.59% under very high accretion. The shoreline behavior was calculated based on the classification scheme used by Naga Kumar [35]. Notably, in Thiruvallur and Chennai, there is the presence of manmade structures (e.g., ports, sea walls, and mitigation-related structures) that can cause shoreline change (both erosion and accretion) in either way.

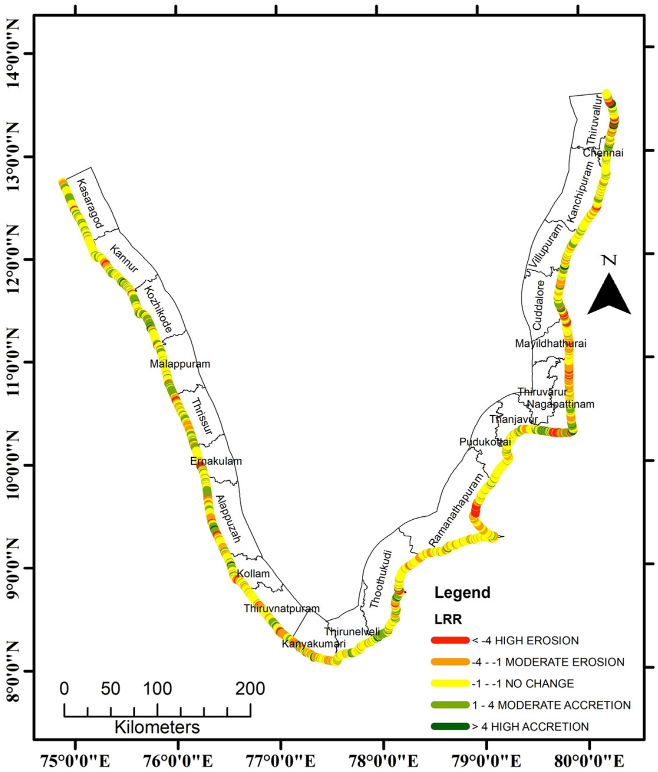

Figure 6. Shoreline behavior map based on Linear Regression Rate method on DSAS.

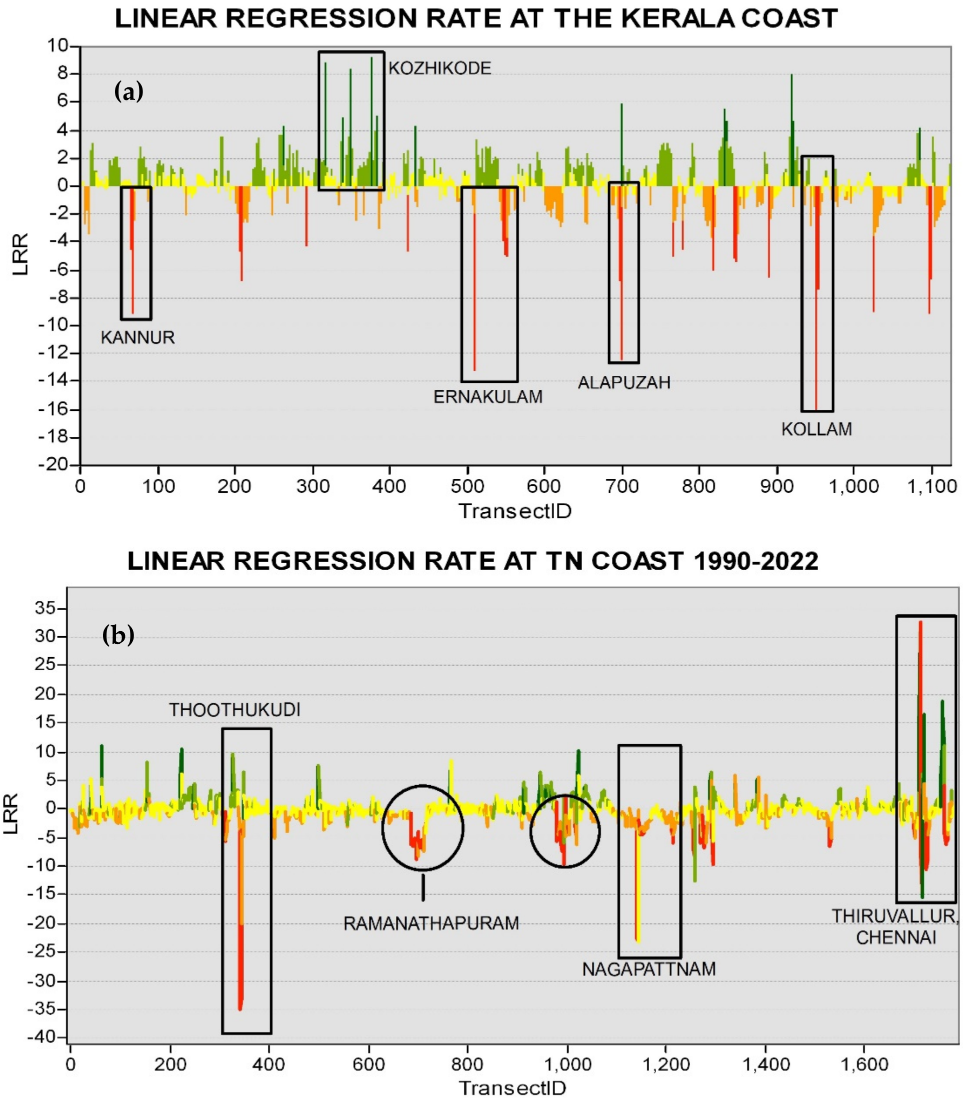

Figure 7. Representation of the shoreline movement of the coasts as represented by LRR (1900–2022). (**a**) LRR at the Kerala coast, and (**b**) LRR at the Tamil Nadu coast. Red and green colors represent erosion and accretion, respectively, orange indicates moderate erosion, light green indicates moderate accretion, and yellow indicates no change. Black circle and rectangle indicate areas with smaller and higher changes, respectively.

4.2. Socio-Economic Parameters

4.2.1. Regional Population Density

In the population density map (Figure 8a), it can be seen that the regions of Thiruvallur, Chennai, and Kanyakumari on the east coast are highly populated, and the regions remaining on the east coast are less populated. The Ramanathapuram region falls under the lowest population density, as per the standard class intervals used for mapping population density. The SEDAC-based shapefiles of different built-up classes were used to generate a built-up density map. According to the map, there is a more concentrated built-up area on the west coast, especially in Malappuram, Thrissur, and Kozhikode. Other than Kasaragod, all of the areas are in the moderate built-up index category, whereas the Kasaragod area is in the low-density category.

4.2.2. Regional Built-Up Area and Urban Density

According to the SEDAC data, Chennai is the densest urban area. Kanyakumari is semi-urban, whereas the other coastal regions on the east coast are rural. On the other hand, the density of urban built-up was identified as moderate in the five districts of the Kerala coast (Figure 8b). Kasaragod district is rural, whereas the other three districts, namely, Ernakulam, Thrissur, and Kannur districts are urban. However, the density of the built-up is moderate, which can be seen in the districts of Alappuzha, Kollam, and Thiruvananthapuram on the West coast (Figure 8c).

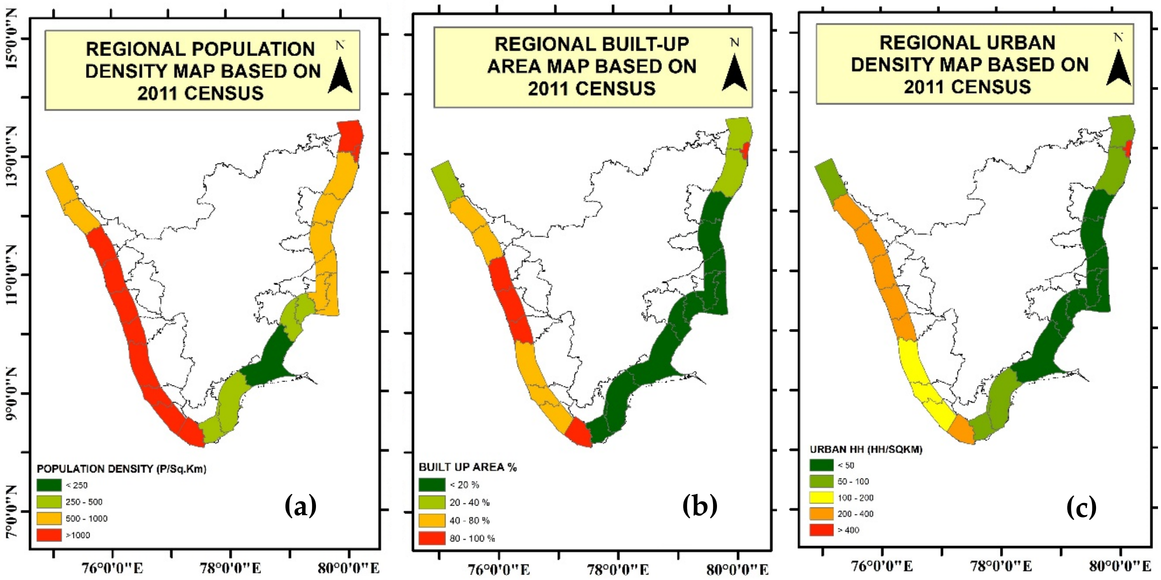

Figure 8. Population density (**a**), built-up density (**b**), and urban density (**c**) based on the 2011 census.

4.3. Physical Vulnerability Assessment

The physical vulnerability map (Figure 9) of the study area was obtained after the complete fuzzy AHP process showed very highly vulnerable areas concerning physical parameters in red, followed by orange for highly vulnerable, yellow for moderately vulnerable, light green for low vulnerability, and dark green for very low vulnerable areas. The area covered under the very highly vulnerable class was about 4345.12 km^2, which accounted for 9.10% of the study area. The second most vulnerable area (i.e., highly vulnerable area) accounted for 8486.40 km^2 occupying 17.77%. The moderately vulnerable class occupies 27.72%, with an area of 13,237.16 km^2, and the low vulnerable area occupies 43.32% of the area (i.e., 20,685 km^2). The least vulnerable area is covered under the very low vulnerable class, with an area of 2.08% (or 994.75 km^2).

Table 6. Comparative assessment of coastal parameters, processes, and their impacts.

Parameter	Classes	Tamil Nadu Coast (km^2)	%	Kerala Coast (km^2)	%
Geomorphology	Coastal plains	4257.29	13.51	2395.23	12.53
	Deltaic plains	8509.73	27.00	494.24	2.59
	Flood plains	1712.55	5.43	787.62	4.12
	Waterbody	3112.13	9.87	432.03	2.26
	Pediment–pediplain complex and hills	13,928.00	44.19	15,009.70	78.51
Sea level rise	<1.8 mm	25,000.50	79.24	2874.99	14.92
	1.81–2.25 mm	6548.64	20.76	16,394.00	85.08
Significant wave height	<0.3 m	9153.76	29.06	19,071.30	100.00
	0.3–0.6 m	19,333.40	61.37	-	0
	0.6–0.9 m	3017.09	9.58	-	0

Table 6. *Cont.*

Parameter	Classes	Tamil Nadu Coast (km^2)	%	Kerala Coast (km^2)	%
Physical vulnerability	Very low	638.05	2.10	404.50	2.35
	Low	6650.20	21.93	13,983.20	81.08
	Moderate	10,734.20	35.40	2454.54	14.23
	High	8047.80	26.54	404.46	2.35
	Very high	54.07	14.03	-	0
Social vulnerability	Very low	8486.12	18.70	-	0
	Low	14,078.60	31.02	2100.32	12.15
	Moderate	5111.56	11.26	143.31	0.83
	High	9822.65	21.65	9782.78	56.61
	Very high	7881.63	17.37	5254.76	30.41
Overall vulnerability	Very low	968.88	3.22	497.42	2.90
	Low	10,869.96	36.13	2015.82	11.73
	Moderate	8630.94	28.69	9430.49	54.89
	High	7421.68	24.67	3691.11	21.48
	Very high	2194.55	7.29	1545.12	8.99
Shoreline behavior	High accretion	302.63 km	31.91	316.26 km	56.57
	High erosion	591.55 km	62.38	242.82 km	43.43
	Very high erosion	54.07 km	5.70	-	0

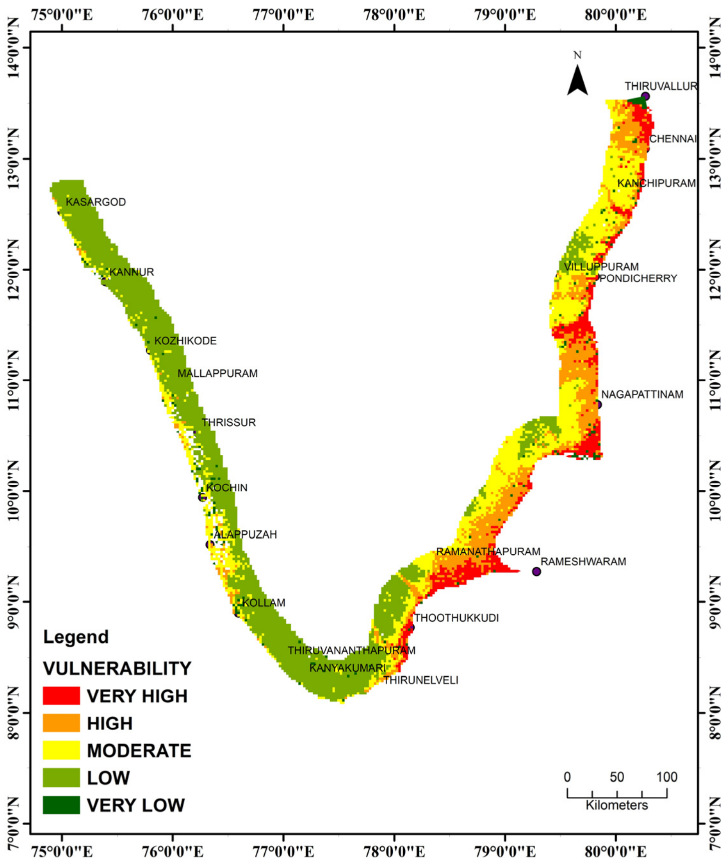

Figure 9. Displays the physically vulnerable areas in five classes, namely, very low, low, moderate, high, and very highly vulnerable. The details are shown in Table 6.

From the map generated (Figure 9), it can be interpreted that the east coast is more vulnerable because of its physical terms, such as geomorphology, slope, elevation, significant wave height, tidal range, and shoreline behavior. In the coastal belt of Tamil Nadu, except for Kanyakumari and some parts of Thoothukudi, the entire on-shore area is classified under very high and highly vulnerable regions. On the west coast, some parts of southern and central Kerala, as well as some regions in northern Kerala, were under high and moderate classes of vulnerability. This happened because on the west coast, except for the rise in sea level, all other factors were resistant to coastal processes.

The elevation is high, and the slope is lower on the west coast than on the east coast. The wave height is less compared to the east and, more importantly, the absence of deltaic and flood plains all along the coast because of a smaller number of large rivers flowing towards the Arabian Sea. The bathymetry is also stable along the west coast compared to the east coast.

4.4. Social Vulnerability Assessment

The social vulnerability map (Figure 10) of the study area showed the very highly vulnerable classes in red color and highly vulnerable in orange, followed by moderately vulnerable in yellow color, low vulnerability in light green, and very low vulnerability in dark green colors. On the east coast, the regions of Chennai and Kanyakumari were shown to be socially very highly vulnerable, as they have a high concentration of households and heavy built-up density, and already there are conditions worsened due to physical vulnerability.

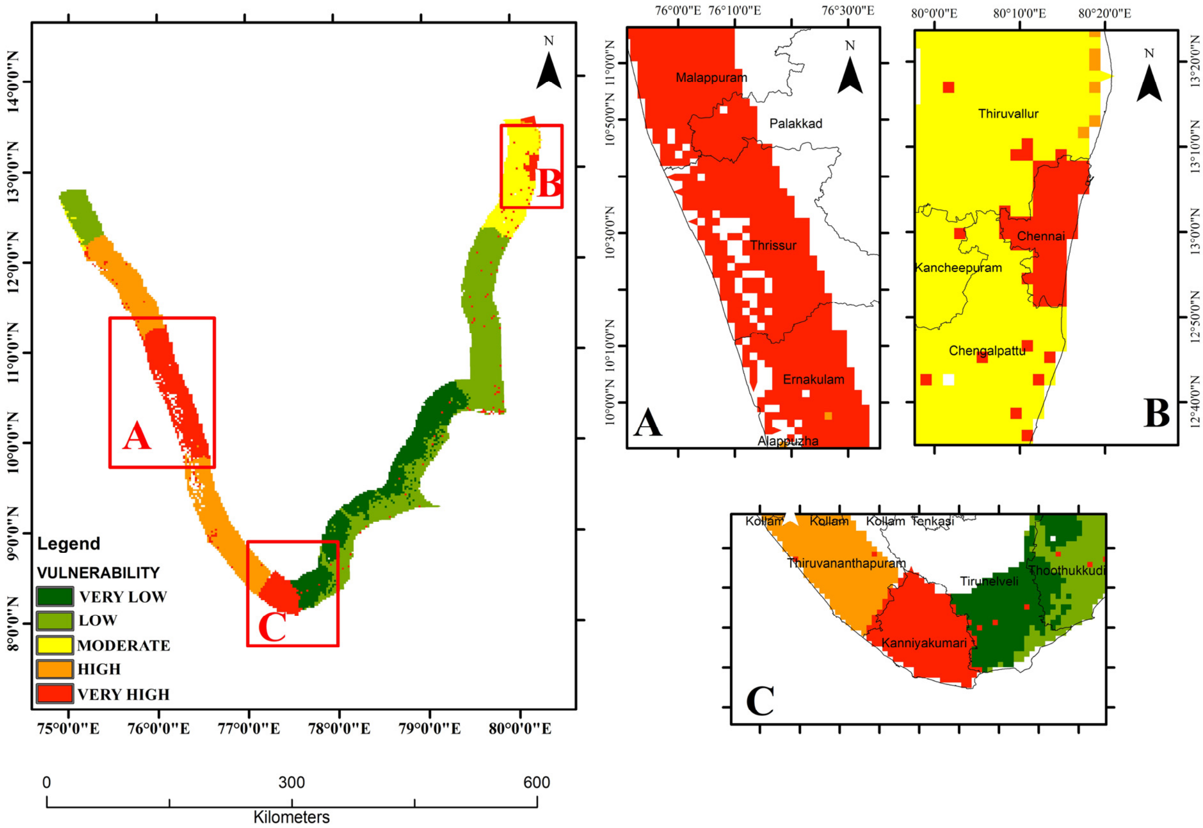

Figure 10. Displays the social vulnerability along the west and east coast in five classes from very low to very high. The highly affected regions such as Chennai, Kanyakumari, Malappuram, Thrissur, and Ernakulam are highlighted. (**A**) shows the very high vulnerable areas of Kerala coast, (**B**) depicts parts of highly vulnerable areas of Chennai and Puducherry and (**C**) shows the very highly vulnerable coastal district of Kanyakumari.

On the east coast, the regions of Malappuram, Thrissur, and Alappuzha were classified as very highly vulnerable, and some parts of Kollam were also under the very high class of vulnerability. The majority of the west coast is under the classes of highly vulnerable concerning social vulnerability, whereas the east coast is less socially vulnerable when compared to the West.

4.5. Overall Vulnerability Assessment

Figure 11 depicts an overall vulnerability that was obtained by averaging both the physical and socially vulnerable outputs. The averaging method has also been applied in previous studies [17,49,52–56]. However, a geometric mean (i.e., the square root of the product) could be another way of combining the two scores with an average. In this study, both methods have resulted in similar patterns in the overall vulnerability map. The overall vulnerability map based on the average method was more accurate. It revealed that the Thiruvallur Chennai, Kanchipuram, Cuddalore, and Nagapattinam regions on the east coast were very highly vulnerable. On the west coast, the Malappuram, Thrissur, Ernakulam, Alappuzha, and Kollam regions were identified as highly vulnerable. The area-wise statistics are shown in Table 6.

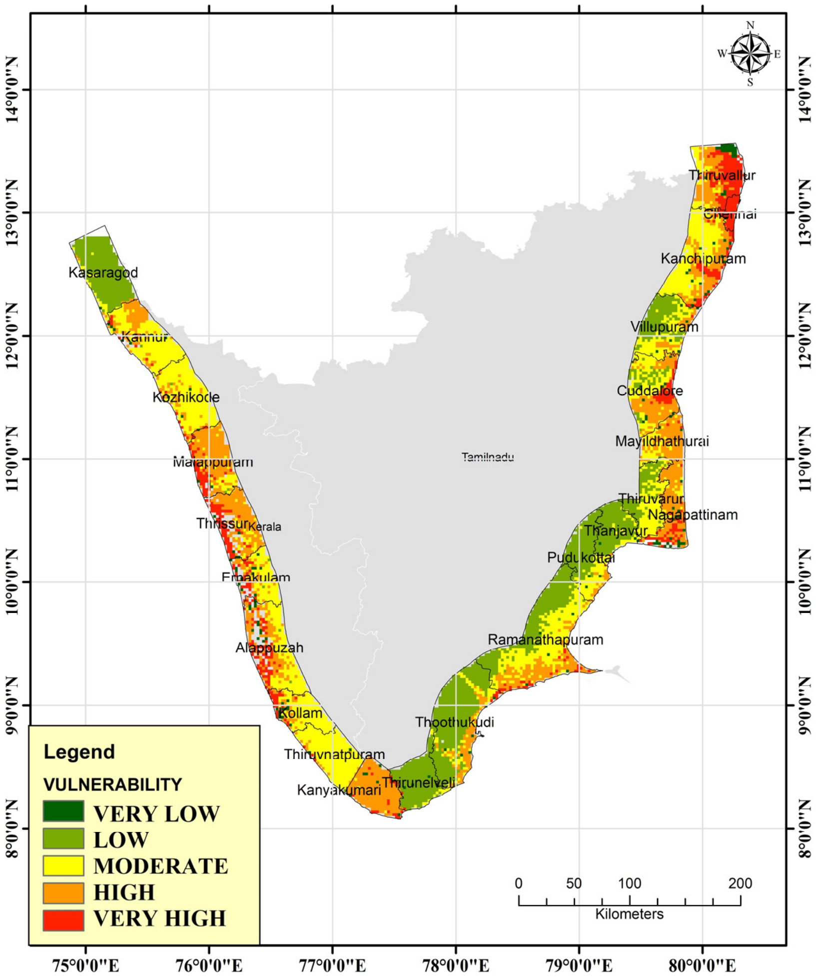

Figure 11. Displays the overall vulnerability along the west and east coasts in five classes from very low to very high. The area-wise statistics are presented in Table 6.

4.6. Comparative Assessment between Tamil Nadu and Kerala Coasts

This section deals with the interpretation and statistical analysis of the data interpreted from different maps. In this present study, we compared coastal changes by including both physical and socio-economical parameters. This study has proven the reasons behind the variability between the east and west coasts using different techniques and considering different parameters.

The parameters considered for the comparative assessment are as follows: (i) geomorphological landforms on both coasts; (ii) areas affected by sea level rise between both coasts; (iii) sea wave height affecting the area between both coasts; (iv) shoreline behavior along both coasts; (v) physical vulnerability area statistics of both regions; (vi) social vulnerability area statistics of both regions and overall vulnerability statistics. A comparison between both coasts is shown in Table 6.

The area under the coastal plains is around 2395 km^2 in Kerala and about 4257 km^2 in Tamil Nadu, forming 12.5% and 13.5% of the Kerala and Tamil Nadu study regions, respectively, as vulnerability-prone areas. Most of the highly vulnerable areas concerning physical vulnerability are covered by coastal plains. Apart from the coastal plains, the western part has 78.51% pediment–pediplain complex hills, 4.12% flood plains, 2.59% deltaic plains, and 2.26% water bodies. On the other hand, in the eastern part of the study area, 44.19% is covered by pediment–pediplain complexes and hills, followed by deltaic plains at 27%, waterbodies at 9.87%, and flood plains at 5.4%. The coastal and deltaic plains are more vulnerable to coastal processes [32]. Tamil Nadu has more area under these two classes, making it more vulnerable than Kerala. The sea level rise is classified into two classes: less than 1.8 mm and more than 1.8 mm. The class < 1.8 mm accounts for about 79% of the Tamil Nadu coast and 15% of the Kerala coast. The class ranging from 1.8 to 2.25 mm was found to be around 20.76% and 85% for the Tamil Nadu and Kerala coasts, respectively. It can be stated that the sea level rise affects the Kerala coast more than the Tamil Nadu coast.

The entire study area has been affected by waves up to 0.9 m in height. The Kerala coast experienced an average wave height of less than 0.3 m. About 29% of the Tamil Nadu coast experienced waves of below 0.3 m, 61.3% area was affected by waves of 0.3–0.6 m, and 9.57% area was affected by larger waves ranging from 0.6 to 0.9 m in the past 30 years. The shoreline behavior, which was estimated based on LRR by DSAS, showed that 56.5% of Kerala's shoreline was under high accretion, and 43.43% experienced high erosion. In the case of Tamil Nadu, 62.3% of the shoreline exhibited high erosion, 31.9% shoreline was under accretion, and 5.70% was very highly eroded.

Based on the physical parameters, the vulnerability map showed that 9.10% of the study area is under the very highly vulnerable class, occupying 4345 km^2. It includes both Tamil Nadu and Kerala. On the eastern side, around 14% of the area falls under the very highly vulnerable, followed by the highly vulnerable area at 26.54%, moderately vulnerable at 35.40%, low vulnerability at 21.9%, and very low vulnerability at 2.10%. The western part accounts for a negligible area under the very high vulnerability class, 2.35% in the highly vulnerable class, 14.23% in the moderate class, 81.08% in the low vulnerability class, and 2.35% in the very low vulnerability class. As discussed earlier, the social vulnerability was estimated after considering population density, household, and urban densities, along with the physical vulnerability as input parameters. Based on social vulnerability, nearly 9.5% of the entire study area was found to be very highly vulnerable, 22.5% as highly vulnerable, 11.61% as moderate, 36.9% as low, and 19.2% as very low vulnerable areas. In Tamil Nadu, 16.5% of the area was very highly vulnerable, 20.6% under highly vulnerable, 10.7% under the moderately vulnerable class, 29% under low vulnerability, and 17.5% under the very low vulnerability class. In the Kerala part, the majority of the area was found to be under high vulnerability (56.61%), followed by 30.41% area under very high vulnerability, 12.15% under low vulnerability, and 0.83% under moderate vulnerability. The overall vulnerability was obtained by averaging the physical and social vulnerabilities, and the vulnerability scale ranged from 0 to 0.9. Based on the overall vulnerability map, Thiruvallur, Chennai, Cuddalore, and Nagapattinam in the eastern region were identified under very highly vulnerable conditions, whereas, Malappuram, Thrissur, Ernakulam, Alappuzha, and Kollam were identified under highly vulnerable conditions.

5. Discussion

Coastal areas are always under the influence of some or other coastal forces. Continuous monitoring and improvising of the ground and remotely sensed data make the decision-making process easy and fast. As coasts are interaction zones between different ecosystems, various datasets are required to study specific areas. The coastal vulnerability is usually estimated using various multi-criteria decision-making models, such as CVI, AHP, Fuzzy AHP, TOPSIS, etc. Among them, AHP has been widely used for estimating coastal vulnerability across several coasts globally [57–60]. In these studies, coastal slope, regional elevation, significant wave height, tidal range, shoreline change, geomorphology, sea level changes, population, road network, and LULC were utilized for estimating both physical and social vulnerability. A study by Tahri et al. [5] employed the fuzzy AHP method and estimated coastal vulnerability on the Mohammedia coast situated in Morocco, which divided the coastal ecosystem into three parts, namely, coastal characteristics, coastal forcing, and socio-economic characteristics. Parameters such as LULC, geomorphology, coastal erosion (m/year), and elevation (m) were considered coastal characteristics. The mean wave height (m), sea level rise (mm/year), and mean tidal range (m) were taken as coastal forcing. Distance to the urban area from the coastline (m) was considered a socio-economic parameter. Several other studies have also used similar parameters as those discussed above in the AHP method for deriving coastal vulnerability on different Indian coasts [52,53,56,61]. The present study incorporated three coastal vulnerabilities (i.e., physical, socio-economic, and overall), which were determined using the fuzzy AHP approach. It also incorporated the in situ data, such as Wave Watch III, GLOSS, and SEDAC datasets along with remotely sensed data. Particularly for estimating physical vulnerability, we used geomorphology, regional elevation, slope, mean sea level change, surface significant wave height, and shoreline behavior. These are the parameters that were responsible for changing and rapidly modifying the shorelines of the selected area. Hence, we incorporated the same to estimate the physical vulnerability.

LULC has been used as a socio-economic parameter by Mani Murali [57] and Mahapatra [58], whereas Tahri et al. [5] have considered LULC as a coastal characteristic to estimate physical vulnerability. Moreover, in the present study, LULC was not used as the geomorphology and elevation were already taken into account. In case LULC is weak in geological terms (e.g., salt pans and beaches), such land covers are more vulnerable to continuous processes such as coastal forcing. At the same time, if an area is low elevated and geologically and geomorphologically weak, irrespective of its LULC, it is highly vulnerable. Previous studies on coastal vulnerability over the Indian coast [11,54,62–65] considered the tidal range or spring tide range as a parameter and found large variations in tidal ranges (0.50 m–11.6 m). During this study, it was found that the entire area experienced a similar or equal impact from tides (~1.8 m), due to which the tidal range was not included in the list of parameters used for estimating physical vulnerability.

In this study, a new concept of overall vulnerability has been introduced. It is an average of both physical and social vulnerabilities. So, areas that are both physically and socially highly vulnerable can be considered very highly vulnerable. Furthermore, areas that are socially more and physically less, or vice versa, have been named moderately vulnerable. The areas that fall under low physical and social vulnerability have been automatically categorized under overall low vulnerability areas. The key findings of this study indicate that areas such as Thiruvallur, Chennai, Cuddalore, Nagapattinam, and Ramanathapuram on the east coast, and Malappuram, Ernakulam, Thrissur, and Alappuzha on the west coast are highly impacted and vulnerable due to coastal processes. The inclusion of both remotely sensed and in situ data makes these results more relevant and reliable. In line with our above findings, Mujabar et al. [17], Priya Ranjan et al. [49], and Sankari et al. [55] reported that Thiruvallur, Chennai, and Cuddalore on the Tamil Nadu coast are highly vulnerable, whereas Naga Kumar et al. [47] identified Alappuzha, Ernakulam, Thrissur on the Kerala coast as highly vulnerable due to coastal processes in terms of physical and social perspectives. It is noteworthy to mention that the coarse resolution of Wave Watch III and the limited tide gauge station data in GLOSS-PSMSL can potentially influence the three derived vulnerabilities on the Indian coast. A limitation of the present study is the field verification of the shoreline movement, which is important for improving accuracy. Estimating the surface significant wave height, tidal range, and sea level change with appropriate equipment in selected locations can further enhance the obtained results. Such improvisations are helpful in decision making. Modern artificial intelligence, machine, and deep learning techniques analyze conditions more complex than AHP, fuzzy AHP, and TOPSIS, and derive outputs more swiftly [66]. It is suggested to estimate further changes using such advanced techniques, giving a geospatial outlook.

The adopted framework to estimate vulnerability can be applied over any coast on Earth, with a minor change in selecting the parameters. As the coasts change, there will be a change in affecting coastal forcing, and as a result, the required datasets also change. The wave direction, velocity, wind speed, etc. are typically mapped using satellite data, which are available at both finer and coarser spatial resolutions. In such studies, a finer resolution should be adopted for acquiring accurate vulnerability maps.

6. Conclusions

The sea level is rising along both coasts, but the west coast is experiencing a greater rise compared to the east coast. Although there is some variation in the wave height along the study area, the east coast is more frequently hit by higher wave heights than the west coast. Regions with weak geomorphology, low elevation, low slope, higher sea level rise, wave height, and eroding shores were marked as very highly vulnerable. The east coast is physically more vulnerable and socially less vulnerable. Based on the physical parameters, very high vulnerability classes accounted for 9.1% (4345.12 km^2) of the area. With respect to social and overall vulnerability, the very highly vulnerable class consisted of 16.57% (7881 km^2) of the area. By identifying the vulnerable coasts and their causing forces, it will be easy to take the necessary mitigation steps by the policymakers and the administrators. The results of this coastal vulnerability study can provide integrated coastal zone management, adaptation planning, and building resilient coastal communities. In order to safeguard these coasts from the continuous impact of coastal forcing and reduce the damage, dune rehabilitation, construction of green belts, artificial reefs, and mangrove plantations can be performed along the identified highly vulnerable shores.

Author Contributions: C.S.D., S.T.P., A.C.P. and B.R.P.: Conceptualization, investigation, methodology, software, analysis, visualization, writing—original draft, and writing—review and editing. D.M. and N.K.: Methodology, software, supervision, analysis, visualization, writing—original draft, and writing—review and editing. All authors have read and agreed to the published version of the manuscript.

Funding: This research received no external funding.

Institutional Review Board Statement: Not applicable.

Informed Consent Statement: Not applicable.

Data Availability Statement: In this study, publicly available datasets were analyzed, which can be accessed from the sources provided in Table 2.

Acknowledgments: The authors thank NASA, USGS, APDRC, and SEDAC for providing the data free of cost.

Conflicts of Interest: The authors declare no conflict of interest.

Appendix A

Defuzzified Matrix

	GEO	RE	MSL	SWH	TIDAL R	SM
GEO	1	1.33	3	9	8	8
RE	0.83	1	5	5	8	8
MSL	0.36	0.21	1	3	3	7
SWH	0.11	0.21	0.4	1	3	5
TIDAL R	0.13	0.13	0.4	0.36	1	1.3
SM	0.13	0.13	0.1	0.21	0.8	1
TOTALS	2.56	3	9.9	18.6	24	30

Appendix B

Normalized Matrix						
	GEO	RE	MSL	SWH	SLOPE	SM
GEO	0.39	0.44	0.3	0.48	0.3	0.3
RE	0.33	0.33	0.5	0.27	0.3	0.3
MSL	0.14	0.07	0.1	0.16	0.1	0.2
SWH	0.04	0.07	0	0.05	0.1	0.2
SLOPE	0.05	0.04	0	0.02	0	0
SM	0.05	0.04	0	0.01	0	0

Appendix C

Weights	Weighted Sum	Lambda
0.37066	2.535548	6.840637
0.339141	2.308372	6.806535
0.138219	0.921197	6.664763
0.082198	0.514093	6.254363
0.038915	0.249332	6.407104
0.030868	0.189877	6.151184

Appendix D

Validating Parameters		
Lambda Max	6.520764	
n	6	
RI	1.24	
C I	(L-N/N-1)	0.104153
CR	(CI/RI)	0.083994

References

1. Nayak, S. Coastal Zone Management in India—Present Status and Future Needs. *Geo Spat. Inf. Sci.* **2017**, *20*, 174–183. [CrossRef]
2. Ahmad, H. Bangladesh Coastal Zone Management Status and Future Trends. *J. Coast. Zone Manag.* **2019**, *22*, 466.
3. Davidson-Arnott, R.; Bauer, B.; Houser, C. *Introduction to Coastal Processes and Geomorphology*; Cambridge University Press: Cambridge, UK, 2019; ISBN 9781108424271.
4. Unnikrishnan, A.S.; Kumar, K.R.; Fernandes, S.E.; Michael, G.S.; Patwardhan, S.K. Sea Level Changes along the Indian Coast: Observations and Projections. *Curr. Sci.* **2006**, *90*, 362–368.
5. Tahri, M.; Maanan, M.; Maanan, M.; Bouksim, H.; Hakdaoui, M. Using Fuzzy Analytic Hierarchy Process Multi-Criteria and Automatic Computation to Analyse Coastal Vulnerability. *Prog. Phys. Geogr. Earth Environ.* **2017**, *41*, 268–285. [CrossRef]
6. Masselink, G.; Hughes, M.; Knight, J. *Introduction to Coastal Processes and Geomorphology*; Routledge: Oxfordshire, UK, 2014.
7. Orviku, K.; Jaagus, J.; Kont, A.; Ratas, U. Reimo Rivis Increasing Activity of Coastal Processes Associated with Climate Change in Estonia. *J. Coast. Res.* **2003**, *19*, 364–375.
8. Bird, E. *Coastal Geomorphology: An Introduction*, 2nd ed.; Wiley-Blackwell: Hoboken, NJ, USA, 2008; ISBN 9780470517291.
9. Nicholls, R.J.; Klein, R.J.T. Climate Change and Coastal Management on Europe's Coast. In *Managing European Coasts*; Springer: Berlin/Heidelberg, Germany, 2005; pp. 199–226.
10. Kaliraj, S.; Chandrasekar, N.; Ramachandran, K.K. Mapping of Coastal Landforms and Volumetric Change Analysis in the South West Coast of Kanyakumari, South India Using Remote Sensing and GIS Techniques. *Egypt J. Remote Sens. Space Sci.* **2017**, *20*, 265–282. [CrossRef]
11. Basheer Ahammed, K.K.; Pandey, A.C. Geoinformatics Based Assessment of Coastal Multi-Hazard Vulnerability along the East Coast of India. *Spat. Inf. Res.* **2019**, *27*, 295–307. [CrossRef]
12. Serafin, K.A.; Ruggiero, P.; Barnard, P.L.; Stockdon, H.F. The Influence of Shelf Bathymetry and Beach Topography on Extreme Total Water Levels: Linking Large-Scale Changes of the Wave Climate to Local Coastal Hazards. *Coast. Eng.* **2019**, *150*, 1–17. [CrossRef]
13. Parida, B.R.; Behera, S.N.; Oinam, B.; Patel, N.R.; Sahoo, R.N. Investigating the Effects of Episodic Super-Cyclone 1999 and Phailin 2013 on Hydro-Meteorological Parameters and Agriculture: An Application of Remote Sensing. *Remote Sens. Appl. Soc. Environ.* **2018**, *10*, 128–137. [CrossRef]

14. Basheer Ahammed, K.K.; Pandey, A.C.; Parida, B.R.; Wasim; Dwivedi, C.S. Impact Assessment of Tropical Cyclones Amphan and Nisarga in 2020 in the Northern Indian Ocean. *Sustainability* **2023**, *15*, 3992. [CrossRef]
15. Kumar, V.S.; Pathak, K.C.; Pednekar, P.; Raju, N.S.N.; Gowthaman, R. Coastal Processes along the Indian Coastline. *Curr. Sci.* **2006**, *91*, 530–536.
16. Senapati, S.; Gupta, V. Climate Change and Coastal Ecosystem in India: Issues in Perspectives. *Int. J. Environ. Sci.* **2014**, *5*, 530–543.
17. Sheik Mujabar, P.; Chandrasekar, N. Coastal Erosion Hazard and Vulnerability Assessment for Southern Coastal Tamil Nadu of India by Using Remote Sensing and GIS. *Nat. Hazards* **2013**, *69*, 1295–1314. [CrossRef]
18. O'Regan, P.R. The Use of Contemporary Information Technologies for Coastal Research and Management: A Review. *J. Coast. Res.* **1996**, *12*, 192–204.
19. Pantusa, D.; D'Alessandro, F.; Frega, F.; Francone, A.; Tomasicchio, G.R. Improvement of a Coastal Vulnerability Index and Its Application along the Calabria Coastline, Italy. *Sci. Rep.* **2022**, *12*, 21959. [CrossRef] [PubMed]
20. What Is Coastal Vulnerability Index (CVI)?—Civilsdaily. Available online: https://www.civilsdaily.com/news/what-is-coastal-vulnerability-index-cvi/ (accessed on 21 May 2023).
21. Hasan, M.U.; Drakou, E.G.; Karymbalis, E.; Tragaki, A.; Gallousi, C.; Liquete, C. Modelling and Mapping Coastal Protection: Adapting an EU-Wide Model to National Specificities. *Sustainability* **2022**, *15*, 260. [CrossRef]
22. Klemas, V. Remote Sensing Techniques for Studying Coastal Ecosystems: An Overview. *J. Coast. Res.* **2011**, *27*, 2–17.
23. Ai, B.; Tian, Y.; Wang, P.; Gan, Y.; Luo, F.; Shi, Q. Vulnerability Analysis of Coastal Zone Based on InVEST Model in Jiaozhou Bay, China. *Sustainability* **2022**, *14*, 6913. [CrossRef]
24. Lu, J.; Zhang, Y.; Shi, H.; Lv, X. Coastal Vulnerability Modelling and Social Vulnerability Assessment under Anthropogenic Impacts. *Front. Mar. Sci.* **2022**, *9*, 2038. [CrossRef]
25. Furlan, E.; Pozza, P.D.; Michetti, M.; Torresan, S.; Critto, A.; Marcomini, A. Development of a Multi-Dimensional Coastal Vulnerability Index: Assessing Vulnerability to Inundation Scenarios in the Italian Coast. *Sci. Total Environ.* **2021**, *772*, 144650. [CrossRef]
26. Valis, D.; Hasilova, K.; Forbelska, M.; Pietrucha-Urbanik, K. Modelling Water Distribution Network Failures and Deterioration. In Proceedings of the 2017 IEEE International Conference on Industrial Engineering and Engineering Management (IEEM), Singapore, 10–13 December 2017; pp. 924–928.
27. Mullick, M.R.A.; Tanim, A.H.; Islam, S.M.S. Coastal Vulnerability Analysis of Bangladesh Coast Using Fuzzy Logic Based Geospatial Techniques. *Ocean Coast. Manag.* **2019**, *174*, 154–169. [CrossRef]
28. Pantusa, D.; Saponieri, A.; Tomasicchio, G.R. Assessment of Coastal Vulnerability to Land-Based Sources of Pollution and Its Application in Apulia, Italy. *Sci. Total Environ.* **2023**, *886*, 163754. [CrossRef] [PubMed]
29. Wu, C.; Liu, G.; Huang, C.; Liu, Q.; Guan, X. Ecological Vulnerability Assessment Based on Fuzzy Analytical Method and Analytic Hierarchy Process in Yellow River Delta. *Int. J. Environ. Res. Public Health* **2018**, *15*, 855. [CrossRef] [PubMed]
30. Barzehkar, M.; Parnell, K.E.; Soomere, T.; Dragovich, D.; Engström, J. Decision Support Tools, Systems and Indices for Sustainable Coastal Planning and Management: A Review. *Ocean Coast. Manag.* **2021**, *212*, 105813. [CrossRef]
31. Cao, C.; Cai, F.; Qi, H.; Liu, J.; Lei, G.; Zhu, K.; Mao, Z. Coastal Erosion Vulnerability in Mainland China Based on Fuzzy Evaluation of Cloud Models. *Front. Mar. Sci.* **2022**, *8*, 790664. [CrossRef]
32. Hoque, M.A.-A.; Pradhan, B.; Ahmed, N.; Ahmed, B.; Alamri, A.M. Cyclone Vulnerability Assessment of the Western Coast of Bangladesh. *Geomat. Nat. Hazards Risk* **2021**, *12*, 198–221. [CrossRef]
33. Kuriakose, G.; Sebastian, J. History, Biogeography, Biodiversity and Bioprospecting: Scenario from the Western Ghats. *South Indian J. Biol. Sci.* **2016**, *2*, 292–301. [CrossRef]
34. Hegde, S.; Sharathchandra, K.; Sridhar, K.R. Honey-Producing Bee–Pollen–Vegetation Relationships in the West Coast and Western Ghats of India. *Palynology* **2023**, *16*, 2127957. [CrossRef]
35. Hall, K.R. Commodity Flows, Diaspora Networking, and Contested Agency in the Eastern Indian Ocean c. 1000–1500. *TRaNS Trans-Reg.-Natl. Stud. Southeast Asia* **2016**, *4*, 387–417. [CrossRef]
36. Jayappa, K.S.; Mitra, D.; Mishra, A.K. Coastal Geomorphological and Land-use and Land-cover Study of Sagar Island, Bay of Bengal (India) Using Remotely Sensed Data. *Int. J. Remote Sens.* **2006**, *27*, 3671–3682. [CrossRef]
37. Woodcock, C.E.; Allen, R.; Anderson, M.; Belward, A.; Bindschadler, R.; Cohen, W.; Gao, F.; Goward, S.N.; Helder, D.; Helmer, E.; et al. Free Access to Landsat Imagery. *Science* **2008**, *320*, 1011. [CrossRef] [PubMed]
38. USGS; NASA. *Landsat Data Users Handbook*; USGS and NASA: Reston, VA, USA; p. 8.
39. Farr, T.G.; Rosen, P.A.; Caro, E.; Crippen, R. The Shuttle Radar Topography Mission. *Rev. Geophys.* **2007**, *45*, 2. [CrossRef]
40. Werner, M. Shuttle Radar Topography Mission (SRTM): Experience with the X-Band SAR Interferometer. In Proceedings of the 2001 CIE International Conference on Radar Proceedings (Cat No.01TH8559), Beijing, China, 15–18 October 2001; pp. 634–638.
41. Adilakshmi, L.; Manglik, A.; Thiagarajan, S.; Suresh, M. Crustal Structure of the Indian Plate underneath the Alluvial Plains of the Central Ganga Basin by Broadband Magnetotellurics. *Tectonophysics* **2021**, *802*, 228746. [CrossRef]

42. Tolman, H.L. User Manual and System Documentation of WAVEWATCH III TM Version 3.14. Technical Note, MMAB Contribution. Available online: https://www.google.com.hk/search?q=Tolman+User+Manual+and+System+Documentation+of+WAVEWATCH+III+TM+Version+3.14.+Technical+Note%2C+MMAB+Contribution&ei=7DeJZM_8G8XChwORoqj4Ag&ved=0ahUKEwjPos_M7MH_AhVF4WEKHRERCi8Q4dUDCA4&uact=5&oq=Tolman+User+Manual+and+System+Documentation+of+WAVEWATCH+III+TM+Version+3.14.+Technical+Note%2C+MMAB+Contribution&gs_lcp=Cgxnd3Mtd2l6LXNlcnAQA0oECEEYAFAAWABgAGgAcAB4AIABAIgBAJIBAJgBAKABAqABAQ&sclient=gws-wiz-serp (accessed on 21 May 2023).
43. Duong, T.M.; Ranasinghe, R.; Thatcher, M.; Mahanama, S.; Wang, Z.B.; Dissanayake, P.K.; Hemer, M.; Luijendijk, A.; Bamunawala, J.; Roelvink, D.; et al. Assessing climate change impacts on the stability of small tidal inlets: Part 2- data rich environments. *Mar. Geol.* **2018**, *395*, 65–81. [CrossRef] [PubMed]
44. Merrifield, M.; Aarup, T.; Allen, A.; Aman, A.; Caldwell, P.; Bradshaw, E.; Fernandes, R.M.S.; Hayashibara, H.; Hernandez, F.; Kilonsky, B.; et al. The Global Sea Level Observing System (GLOSS). In Proceedings of the Ocean Obs, Venice, Italy, 25 September 2009; p. 9.
45. Bell, C.; Vassie, J.M.; Woodworth, P.L. POL/PSMSL Tidal Analysis Software Kit 2000 (TASK-2000). In *Permanent Service for Mean Sea Level*; Bidston Observatory: Birkenhead, UK, 1999; p. 20.
46. Gao, J.; Pesaresi, M. Downscaling SSP-consistent global spatial urban land projections from 1/8-degree to 1-km resolution 2000–2100. *Sci. Data* **2021**, *8*, 281. [CrossRef] [PubMed]
47. Naga Kumar, K.C.V.; Deepak, P.M.; Basheer Ahammed, K.K.; Rao, K.N.; Gopinath, G.; Dinesan, V.P. Coastal Vulnerability Assessment Using Geospatial Technologies and a Multi-Criteria Decision Making Approach—A Case Study of Kozhikode District Coast, Kerala State, India. *J. Coast. Conserv.* **2022**, *26*, 16. [CrossRef]
48. Shared Socioeconomic Pathways (SSPs). Available online: https://sedac.ciesin.columbia.edu/data/set/ssp-1-km-downscaled-urban-land-extent-projection-base-year-ssp-2000-2100 (accessed on 25 September 2022).
49. Priya Rajan, S.M.; Nellayaputhenpeedika, M.; Tiwari, S.P.; Vengadasalam, R. Mapping and Analysis of the Physical Vulnerability of Coastal Tamil Nadu. *Hum. Ecol. Risk Assess. Int. J.* **2020**, *26*, 1879–1895. [CrossRef]
50. Arkema, K.K.; Guannel, G.; Verutes, G.; Wood, S.A.; Guerry, A.; Ruckelshaus, M.; Kareiva, P.; Lacayo, M.; Silver, J.M. Coastal Habitats Shield People and Property from Sea-Level Rise and Storms. *Nat. Clim. Chang.* **2013**, *3*, 913–918. [CrossRef]
51. Hadipour, V.; Vafaie, F.; Kerle, N. An Indicator-Based Approach to Assess Social Vulnerability of Coastal Areas to Sea-Level Rise and Flooding: A Case Study of Bandar Abbas City, Iran. *Ocean Coast. Manag.* **2020**, *188*, 105077. [CrossRef]
52. Rajakumari, S.; Minnu, A.; Sarunjith, K.J. Determination of Vulnerable Zones along Brahmapur Coast, Odisha Using AHP and GIS with Validation against Multiple Cyclones. *Environ. Monit. Assess.* **2022**, *194*, 278. [CrossRef]
53. Baig, M.R.I.; Shahfahad; Ahmad, I.A.; Tayyab, M.; Asgher, M.S.; Rahman, A. Coastal Vulnerability Mapping by Integrating Geospatial Techniques and Analytical Hierarchy Process (AHP) along the Vishakhapatnam Coastal Tract, Andhra Pradesh, India. *J. Indian Soc. Remote Sens.* **2021**, *49*, 215–231. [CrossRef]
54. Dwarakish, G.S.; Vinay, S.A.; Natesan, U.; Asano, T.; Kakinuma, T.; Venkataramana, K.; Pai, B.J.; Babita, M.K. Coastal Vulnerability Assessment of the Future Sea Level Rise in Udupi Coastal Zone of Karnataka State, West Coast of India. *Ocean Coast. Manag.* **2009**, *52*, 467–478. [CrossRef]
55. Sankari, T.S.; Chandramouli, A.R.; Gokul, K.; Surya, S.S.M.; Saravanavel, J. Coastal Vulnerability Mapping Using Geospatial Technologies in Cuddalore-Pichavaram Coastal Tract, Tamil Nadu, India. *Aquat. Procedia* **2015**, *4*, 412–418. [CrossRef]
56. Ghosh, S.; Mistri, B. Assessing Coastal Vulnerability to Environmental Hazards of Indian Sundarban Delta Using Multi-Criteria Decision-Making Approaches. *Ocean Coast. Manag.* **2021**, *209*, 105641. [CrossRef]
57. Mani Murali, R.; Ankita, M.; Amrita, S.; Vethamony, P. Coastal Vulnerability Assessment of Puducherry Coast, India, Using the Analytical Hierarchical Process. *Nat. Hazards Earth Syst. Sci.* **2013**, *13*, 3291–3311. [CrossRef]
58. Mahapatra, M.; Ramakrishnan, R.; Rajawat, A.S. Coastal Vulnerability Assessment Using Analytical Hierarchical Process for South Gujarat Coast, India. *Nat. Hazards* **2015**, *76*, 139–159. [CrossRef]
59. Le Cozannet, G.; Garcin, M.; Bulteau, T.; Mirgon, C.; Yates, M.L.; Méndez, M.; Baills, A.; Idier, D.; Oliveros, C. An AHP-Derived Method for Mapping the Physical Vulnerability of Coastal Areas at Regional Scales. *Nat. Hazards Earth Syst. Sci.* **2013**, *13*, 1209–1227. [CrossRef]
60. Lin, L.; Pussella, P. Assessment of Vulnerability for Coastal Erosion with GIS and AHP Techniques Case Study: Southern Coastline of Sri Lanka. *Nat. Resour. Model.* **2017**, *30*, e12146. [CrossRef]
61. Behera, R.; Kar, A.; Das, M.R.; Panda, P.P. GIS-Based Vulnerability Mapping of the Coastal Stretch from Puri to Konark in Odisha Using Analytical Hierarchy Process. *Nat. Hazards* **2019**, *96*, 731–751. [CrossRef]
62. Kumar, T.S.; Mahendra, R.S.; Nayak, S. Coastal Vulnerability Assessment for Orissa State, East Coast of India. *J. Coast.* **2010**, *26*, 523–534. [CrossRef]
63. Nageswara Rao, K.; Subraelu, P.; Venkateswara Rao, T.; Hema Malini, B.; Ratheesh, R.; Bhattacharya, S.; Rajawat, A.S. Ajai Sea-Level Rise and Coastal Vulnerability: An Assessment of Andhra Pradesh Coast, India through Remote Sensing and GIS. *J. Coast. Conserv.* **2008**, *12*, 195–207. [CrossRef]
64. Sudha Rani, N.N.V.; Satyanarayana, A.N.V.; Bhaskaran, P.K. Coastal Vulnerability Assessment Studies over India: A Review. *Nat. Hazards* **2015**, *77*, 405–428. [CrossRef]

65. Arun Kumar, A.; Kunte, P.D. Coastal Vulnerability Assessment for Chennai, East Coast of India Using Geospatial Techniques. *Nat. Hazards* **2012**, *64*, 853–872. [CrossRef]
66. Kumar, R.; Dwivedi, S.B.; Gaur, S. A Comparative Study of Machine Learning and Fuzzy-AHP Technique to Groundwater Potential Mapping in the Data-Scarce Region. *Comput. Geosci.* **2021**, *155*, 104855. [CrossRef]